

Automated Crawler-Based Ultrasonic Investigation to Monitor the Structural Integrity of Composite Liquid Hydrogen Tanks

SHISHIR KUMAR SINGH and ROGER M. GROVES

ABSTRACT

Inspection of composite liquid hydrogen tanks (LH2) for aviation is very challenging using existing non-destructive testing (NDT) technology. This is due to the external insulation layer and limited access to the inside of the tank. New inspection technology is urgently needed for the LH2 tank inspection and maintenance of these LH2 tanks. This work presents the development of a compact high-payload ratio ultrasonic inspection automatic robotic crawler designed for the inspection of the inner curved surfaces of a carbon fiber reinforced polymer (CFRP) composite. The robot is equipped with wheeled locomotion and uses wheel encoders for precise localization on the irregular inner surfaces of the composite LH2 tank. The crawler carries an ultrasonic flaw detector payload housed in a specially designed enclosure, which securely holds a 5 MHz wheel probe for ultrasonic inspection. This study investigates Proportional-Integral-Derivative (PID) tuning for a crawler integrated with an ultrasonic phased array probe, executing straight-line motion on a CFRP composite surface under dynamic conditions at various speeds. The system is designed to operate through tank openings as small as 250-300 mm in diameter, providing a practical solution for challenging inspection scenarios of the LH2 tank.

Shishir Kumar Singh, Department of Aerospace Structures and Materials, Delft University of Technology, Kluyverweg 1, Delft, 2629 HS, The Netherlands
Roger M. Groves, Department of Aerospace Structures and Materials, Delft University of Technology, Kluyverweg 1, Delft, 2629 HS, The Netherlands

INTRODUCTION

Hydrogen has emerged as a promising alternative to traditional fossil fuels, offering significant potential for a more sustainable future [1]. The growing use of composite materials in aerospace has led to the development of increasingly large and complex liquid hydrogen storage (LH2) tank structures [2]. A major obstacle in the development and commercialization of LH2 tanks for aviation is a lack of effective odd space monitoring of fuel leakage through the inner wall of the tank, delamination or debonding of the inner wall material, microcracking of the wall material, and ply drop-off areas which can cause hydrogen leakage [3, 4]. Advances in robotics and computer science have sparked significant interest in applying these technologies to the structural health monitoring (SHM) of inaccessible areas of composite tanks. Automated devices that attach to LH2 storage tanks and move along their surfaces while scanning and inspecting can significantly accelerate the inspection process and reduce human involvement. Recently, crawling devices have emerged as a viable solution for mobile, unconstrained scanning [5]. This includes multimodal rigid robots—such as mobile robots, flying and perching drones equipped with SHM capabilities using pulse-echo and ultrasonic surface waves techniques employing one or two robots [6, 7, 8]. The climbing robotic platform has a low load-carrying capacity, limiting the number of non-destructive evaluation (NDE) sensors that can be incorporated for flaw inspection [7]. Climbing robots require more complex control algorithms than ground-based mobile robots because of their numerous locomotion modes, which include climbing, traversing, attachment, and detachment. With the advancement of 3D printing technology, robotics are increasingly being developed for high payload applications and optimized for specific applications. The materials used have gained widespread adoption due to their enhanced mechanical properties, cost-effectiveness, and ability to meet the requirements of specialized applications [9, 10].

The primary goal of this study was to develop a cost-effective and user-friendly C-scan inspection system that maintains a high payload ratio while accommodating the curvature and complexity of various surfaces. To achieve this, a 3D-printed robotic structure was designed using fused deposition modeling (FDM) with a polyethylene terephthalate glycol (PETG) composite and integrated with a Phased Array Wheel Probe. While the 3-D printed design supports structural flexibility, optimizing the trade-off between inspection time and energy-efficient payload handling remains challenging. This necessitates the development of advanced path planning algorithms, alongside further exploration of incorporating NDE sensors for odd space Structural Health Monitoring (SHM). A key focus of this research reported in this paper is the role of feedback control, specifically the Proportional-Integral-Derivative (PID) controller, which is widely recognized as the cornerstone of control systems. Over 90% of control systems utilize PID due to its effectiveness, though proper implementation requires significant expertise [11]. This study examines PID tuning in the context of a crawler equipped with a phased array probe, performing straight-line path-based motion over a CFRP composite surface under dynamic conditions. Improper tuning can lead to sluggish system response due to increased inertia from high payloads, thereby demanding greater motor power for maneuvering across inclined surfaces.

METHODOLOGY

The robotic crawler is designed to inspect the inner conformal LH2 tank being developed in the COCOLIH2T project. An Olympus phased array wheel probe of 5 MHz is used to inspect composite thin CFRP materials for the C-scan inspection to identify porosity, delamination, and cracks in the CFRP tank structure. The methodology of the sample inspection is shown in Figure 1. The process begins with modelling and preparing the desired design of the crawler, which is then exported in formats for compatibility with the slicing software PrusaSlicer. In this step, the 3D model of robot parts is converted into G-code using slicing software. The model is divided into discrete layers, and essential printing parameters are layer thickness=0.2 mm, printing speed =200 mm/s in the x and y direction, and infill density=50%, which are configured during the slicing stage. The generated G-code is subsequently uploaded or transferred to the 3D printer to commence the fabrication of crawler parts based on FDM. Upon completion, the printed component undergoes post-processing to eliminate surface imperfections and ensure structural integrity. This post-processing step also aids in preparing the assembly of subparts for its intended robotic application. The structure is attached to a gear motor (M1 and M2) with a 43.8:1 metal gearbox and an integrated quadrature encoder that provides a resolution of 700 counts per revolution of the gearbox's output shaft. Hence calculated, each encoder count corresponds to ~0.224 mm of linear travel accuracy for the crawler wheel. In this work, an encoder was used to calculate the 3D position and performed PID tuning to set the straight-line motion of the ultrasonic probe. A real-time processing system then converts this global localization information into standard encoder signals, ensuring compatibility with any ultrasonic system. This motor is intended for use at 1- 24 V using motor driver (L298N), though the motor can begin rotating at voltages as low as 1V. A higher payload-to-weight ratio of 3-5:1 is targeted for better efficiency. A PID controller is employed to regulate the motor (M1 and M2) speeds, while an encoder is used to estimate the robot's position based on initial and target locations as shown in Figure 2. The system is powered by a voltage regulator of max 15 V supply and controlled by an ATmega2560 microcontrollers. The proposed inspection methodology is given below in Figure 1. The tires of the ultrasonic wheel probe are filled with water and are made of aqualene material which provides high-quality, immersion-like ultrasonic testing. Minimal coupling is required to achieve excellent signal quality, even in difficult scanning situations (acceleration or deceleration) or surface roughness.

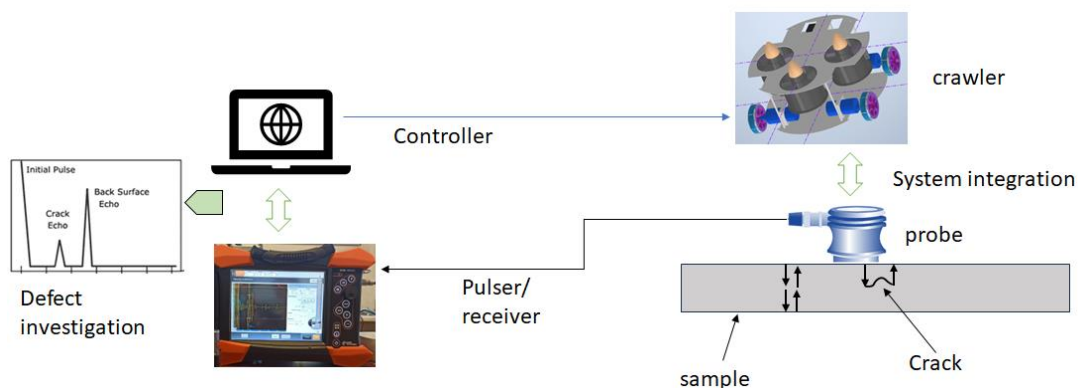


Figure 1. Schematic testing diagram of the sample inspection.

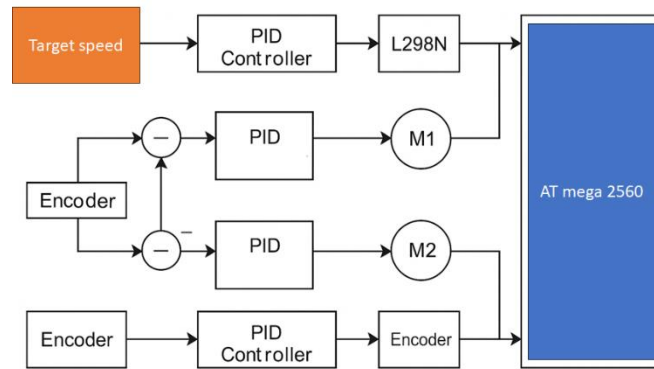


Figure 2. Block diagram of a PID control system for motors.

EXPERIMENTAL SETUP AND RESULTS

The developed non-destructive inspection (NDI) system will be capable of inspecting demonstrator LH2 tanks post-manufacturing for their structural integrity. The crawler will be inserted from the top opening (250-300 mm in diameter) of the inner tank. The NDI crawler control system for the work describe in this paper, was tested on a curved panel of 4.5 mm thickness made of CFRP with a 131.5 mm x 131.5 mm cross-section and radius of 240 mm, having a rough surface and wrinkle. The test is performed on the remote operation using a controller for precise control in path-following for predefined inspection path/patterns which can be longitudinal or transverse along the length of the inner tank—more specifically single unidirectional scan to be performed with a 50 mm coverage length of probe. The process will be repeated till complete the whole inner tank area. In this work, an encoder was used to determine the 3D position, and PID tuning was performed to achieve the straight-line motion of the ultrasonic probe. A real-time processing system then converts this global localization information into standard encoder signals, ensuring compatibility with any ultrasonic system. The robotic crawler with a phased array wheel probe of 5 MHz, PID tuning response study on the curved CFRP sample inclined up to ± 45 degrees as shown in figure 3. This is to check the compatibility of the inspected surface (finish) with the crawler movement system, especially for problems such as slippage and other adhesion problems. Experimental evaluations indicate that with PID parameters set to $K_p = 0.6$, $K_i = 0.5$, and $K_d = 0.03$, the robot achieves smooth and accurate motion. PID Implications at 4-4.5:1 ratio since wheel probe weight is more than 1.5 kg when filled with water. However, note that optimal PID values are used for varying speed/payload during climbing up or down on curved surfaces. When testing a system with no load, the PID might look to be functioning well, but when you add a real payload, the motor might take longer to reach the target speed, overshoot less or more depending on friction and control drift due to uncorrected steady-state error.

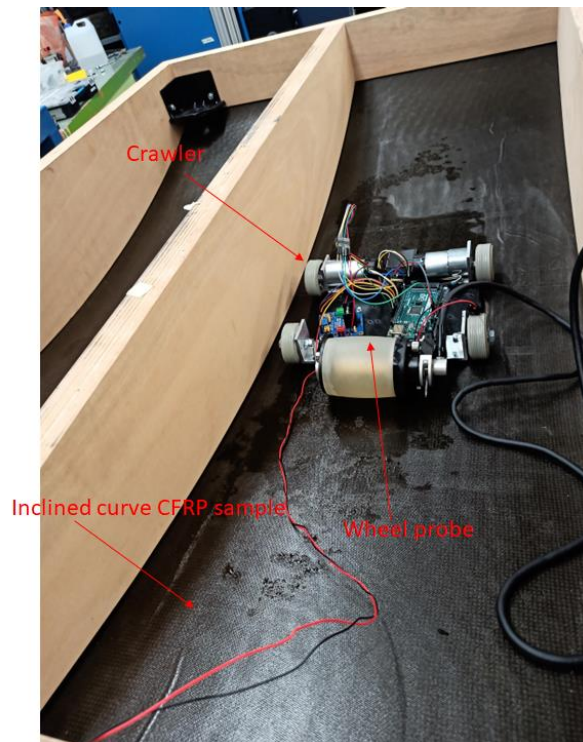


Figure 3. Tested C-scan probe with crawler and CFRP sample.

The system's performance was evaluated by inspecting with various scanning rates (low = 20 RPM = 52 mm/s, medium = 40 RPM = 104 mm/s, and high = 60 RPM = 156 mm/s), demonstrating both its versatility and limitations with the ultrasonic probe, as the behavior of a PID controller on a crawler wheel changes with speed. This variation is primarily due to shifts in system dynamics, non-linearities, and control resolution limits. At low speeds, rolling friction, and static friction play a dominant role, whereas at high speeds, inertia becomes more influential. Additionally, at very low speeds, encoders may struggle to detect small movements accurately, resulting in noisy or imprecise feedback. Conversely, at high speeds, encoder counts may be missed or sampling delays may occur, leading to errors in velocity estimation. At a target speed of 60 RPM for M1 as shown in Figure 4 (a, b), the actual speed eventually stabilizes. The system is stable overall, with a slightly aggressive yet smooth rise, minimal overshoot, and stable tracking with a very small ripple. In contrast, M2 at 60 RPM reaches a stable state with no overshoot or oscillation, though it exhibits a slight steady-state error, stabilizing at approximately 58–59 rpm. The response at 40 rpm is particularly well-tuned, striking a good balance among K_p , K_i , and K_d ; these PID values work optimally at this setpoint as shown in Figure 4 (c, d). For M2, the response also features a smooth rise to the setpoint, with very minimal overshoot and stable performance close to the target. At 20 RPM, the M1 response appears well-tuned, with negligible operational oscillation and a nicely damped response, resulting in a very small, acceptable steady-state error. However, M2 exhibits a fast response accompanied by a significant initial overshoot and persistent oscillation with moderate steady-state error. Overall, the 40 rpm response is the best tuned among the three speeds, delivering a fast, smooth, and accurate performance. This suggests that the PID constants ($K_p =$

0.6, $K_i = 0.5$, $K_d = 0.03$) are optimal for the speed range of 52 mm/s to 104 mm/s ultrasonic inspection.

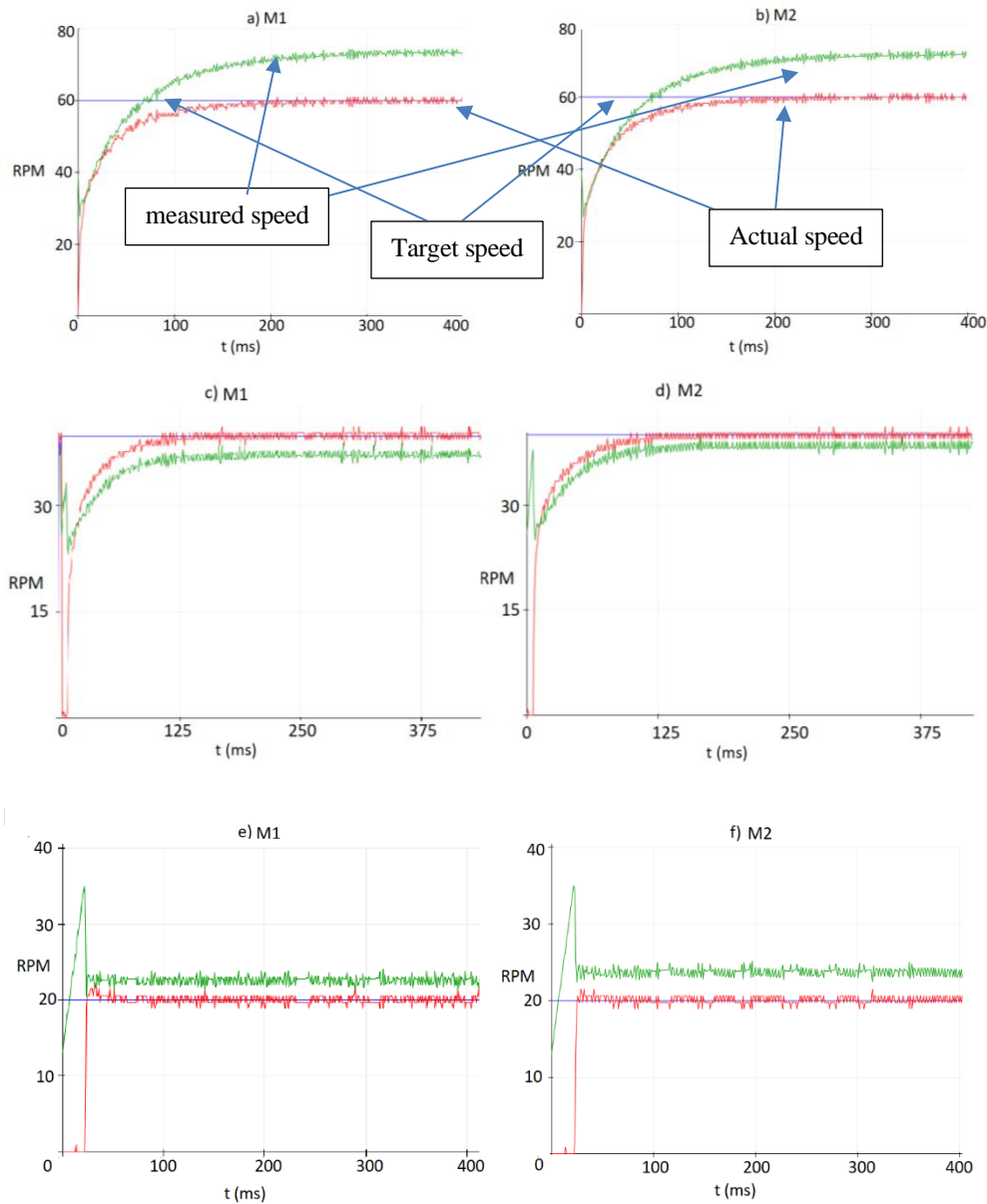


Figure 4. PID tuned response of the both motors at (a, b) 60 RPM, (c, d) 40 RPM, and (e, f) 20 RPM.

The experimental findings demonstrate that the PID controller effectively reduces steady-state inaccuracy and remains resilient to various disturbances in the DC motor system. Manual trial-and-error tuning is safer, more intuitive, and more adaptable for DC motor control, whereas the Ziegler–Nichols method provides a quick starting point but tends to be overly aggressive, often resulting in overshoot, persistent buzzing, or outright instability as shown in Figure 5 for 20 RPM.

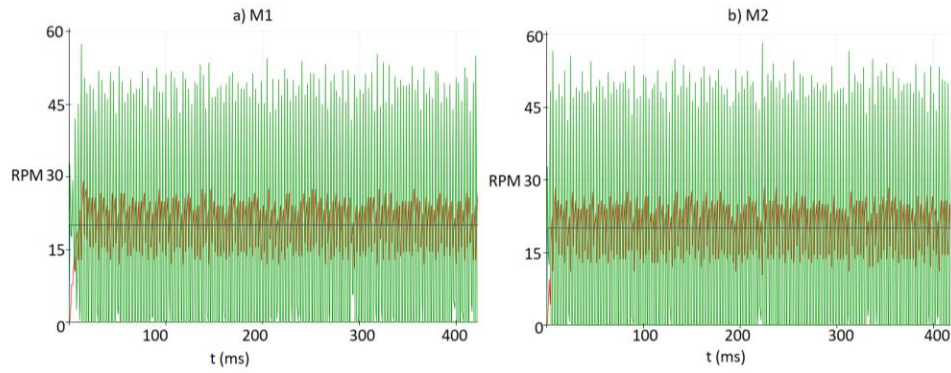


Figure 5. PID tuned response using Ziegler–Nichols method of the both motors at lower speed 20 RPM.

CONCLUSION

This work presents a compact, high-payload ratio robot crawler specifically developed to overcome the limitations of existing NDT techniques for inspecting liquid hydrogen (LH₂) storage tanks. Designed to navigate the complex, curved surfaces of composite LH₂ tanks, the crawler integrates precise wheel-encoder-based localization and an ultrasonic probe system for advanced C-scan imaging for accurate defect detection. Its ability to operate through small access points (250–300 mm) and adapt to various speeds e.g. 20, 40, and 60 RPM conditions. PID control tuned via the trial and error method demonstrates its practical smooth application and robustness. Experimental results confirm the effectiveness and superiority of the proposed control scheme at various speeds particularly 40 RPM and below, making this system a promising solution for efficient and reliable LH₂ tank inspection. Tuning PID with a realistic payload attached as the same one will be used during LH₂ tank inspection. In future work, the ultrasonic inspection focused on the inverted movement of the crawler with probe load-carrying capacity and assessing the defect position in the inner tank (57 kg L) with a volume of 1200l.

ACKNOWLEDGMENT

This research was conducted as part of the Horizon EU Clean Hydrogen COCOLIH2T project under Grant Agreement No. 101101404. The project is supported by the Clean Hydrogen Partnership and its members. Views and opinions expressed are however those of the author(s) only and do not necessarily reflect those of the European Union or Clean Hydrogen Joint Undertaking. Neither the European Union nor the granting authority can be held responsible for them.

REFERENCES

1. Muradov, N. Z., & Veziroğlu, T. N. 2008. "Green path from fossil-based to hydrogen economy: an overview of carbon-neutral technologies." *International Journal of Hydrogen Energy*, 33(23), 6804-6839.
2. Yin, L., Yang, H., & Ju, Y. 2024. "Review on the key technologies and future development of insulation structure for liquid hydrogen storage tanks," *International Journal of Hydrogen Energy*, 57, 1302-1315.
3. Chi, G., Xu, S., Yu, D., Wang, Z., He, Z., Wang, K., & Zhou, Q. 2024. "A brief review of structural health monitoring based on flexible sensing technology for hydrogen storage tank," *International Journal of Hydrogen Energy*, 80, 980-998.
4. Séguin-Charbonneau, L., Walter, J., Thérout, L. D., Scheed, L., Beausoleil, A., & Masson, B. 2021. "Automated defect detection for ultrasonic inspection of CFRP aircraft components," *NDT & E International*, 122, 102478.
5. Tian, Y., Chen, C., Sagoe-Crentsil, K., Zhang, J., & Duan, W. 2022. "Intelligent robotic systems for structural health monitoring: Applications and future trends," *Automation in Construction*, 139, 104273.
6. Gucunski, N., Basily, B., Kim, J., Yi, J., Duong, T., Dinh, K., & Maher, A. 2017. "RABIT: Implementation, performance validation and integration with other robotic platforms for improved management of bridge decks," *International Journal of Intelligent Robotics and Applications*, 1, 271-286.
7. Xu, F., Wang, X., & Wu, H. 2012. "Inspection method of cable-stayed bridge using magnetic flux leakage detection: principle, sensor design, and signal processing," *Journal of Mechanical Science and Technology*, 26, 661-669.
8. Liu, Y. F., Nie, X., Fan, J. S., & Liu, X. G. 2020. "Image-based crack assessment of bridge piers using unmanned aerial vehicles and three-dimensional scene reconstruction," *Computer-Aided Civil and Infrastructure Engineering*, 35(5), 511-529.
9. Delda, R. N. M., Basuel, R. B., Hacla, R. P., Martinez, D. W. C., Cabibihan, J. J., & Dizon, J. R. C. 2021. "3D printing polymeric materials for robots with embedded systems," *Technologies*, 9(4), 82.
10. Alarifi, I. M. 2023. "PETG/carbon fiber composites with different structures produced by 3D printing," *Polymer Testing*, 120, 107949.
11. Singh, I. 2024. "Control Schemes for DC Motors in Electric Drives," Pencil.